Electronic and magnetic properties of α-MnO_2 from *ab initio* calculations

Y. Crespo and N. Seriani
The Abdus Salam ICTP, Strada Costiera 11, I-34151 Trieste, Italy
(Received 25 July 2013; revised manuscript received 18 September 2013; published 31 October 2013)

α-MnO_2, an active catalyst for oxygen reduction and evolution reactions, has been investigated using *ab initio* calculations with different exchange-correlation functionals: the generalized-gradient approximation in the version of Perdew, Burke, and Ernzerhof (PBE), PBE + U, and hybrid functionals. Both hybrid functionals and PBE + U ($U \geqslant 2.0$ eV) fail to capture the antiferromagnetic (AFM) ground state found experimentally, and a ferromagnetic configuration has the lowest energy. An AFM ground state is then recovered when using PBE or PBE + U ($U \leqslant 1.6$ eV). Interestingly, a reduction of the gap is observed at increasing values of the U parameter. We offer a qualitative explanation for the change in the calculated ground state employing the results for the electronic structure and physical arguments similar to those exposed in the Goodenough-Kanamori-Anderson rules. It is argued that the p_z orbital of oxygen atoms with sp^2 hybridization plays a fundamental role in the superexchange AFM interaction and in the reduction of the gap.

DOI: 10.1103/PhysRevB.88.144428 PACS number(s): 71.15.Mb, 71.15.Nc, 72.20.Jv, 77.84.Bw

I. INTRODUCTION

Manganese oxides are materials with very complex electronic and magnetic properties, due to the presence of the localized 3*d* states of the manganese ions. As a result, they display a large variety of phases, from antiferromagnetic (AFM) to helical order.[1–4] This represents a challenge for first-principles simulation methods based on density functional theory (DFT), and it is often necessary to employ post-DFT methods, e.g., hybrid functionals. Still, it is unclear which level of theory is necessary for a satisfactory description; in addition, understanding the reasons behind the diverse results obtained by different exchange and correlation functionals could help rationalizing these discrepancies and shed light on their behavior in Mn oxides.

In this work, we have investigated the electronic and magnetic properties of bulk α-MnO_2 using *ab initio* calculations with different exchange-correlation functionals: the generalized-gradient approximation in the version of Perdew, Burke, and Ernzerhof (PBE),[5] PBE + U, and hybrid functionals. This material has recently drawn considerable attention as a catalyst for lithium-air batteries[6–12] because it is an efficient and relatively cheap catalyst for the oxygen reduction reaction.[11,13–16] Moreover, it finds also applications in catalysis, molecular/ion sieves, chemical sensors, and electrode materials for lithium-ion batteries. Furthermore, it has been shown that α-MnO_2 catalyzes a variety of oxidation reactions, such as the oxidation of ammonia with NO (Ref. 17) and that of methane[18] in presence of visible light or water.[19]

Recently, bulk properties of α-MnO_2 were investigated by DFT (Ref. 20) using the PBEsol + U (Ref. 21) ($U_{\text{eff}} = U - J = 1.6$ eV) functional. They found this method to yield an AFM ground state and a band gap of 1.3 eV. Additionally, the capture of lithium in this material was studied using first-principles calculations by Ling *et al.*[22] They used the PBE + U ($U_{\text{eff}} = 3.9$ eV) approximation for the exchange-correlation functional. In these studies, post-DFT methods are used to investigate this material. Nevertheless, the selection of the functional for exchange and correlation and the value of best suiting U_{eff} can only be achieved by a careful study of the influence of these factors on the electronic and magnetic properties. This was precisely the aim of the work done by Franchini *et al.*[1] where four manganese oxides, MnO, α-Mn_2O_3, Mn_3O_4, and β-MnO_2, were studied within the spin-polarized DFT method. They showed that, even when DFT has limitations in describing this type of materials, hybrid functionals such as Heyd-Scuseria-Ernzerhof[23,24] (HSE) seem to be more suitable to study these oxides.

In this work, we have investigated the electronic and magnetic properties of bulk α-MnO_2 by using different approximations for the exchange-correlation functional [PBE, PBE + U ($U_{\text{eff}} = 1.6$, 2.0, and 3.9 eV) and hybrid functionals]. Experimentally, this compound is found to have an AFM configuration at low temperature.[2] Nevertheless, our calculations show that, when PBE + U ($U \geqslant 2.0$ eV) or hybrid functionals are used, the obtained ground state is ferromagnetic (FM). Interestingly, also the electronic band gap starts to decrease for $U_{\text{eff}} \geqslant 2.0$ eV. An AFM configuration is then recovered if the approximations PBE and PBE + U ($U_{\text{eff}} \leqslant 1.6$ eV) are used. This change was also found in other manganese compounds in the previous study done by Franchini *et al.*[1] It was shown that the predicted magnetic ground state of the compounds α-Mn_2O_3 and β-MnO_2 changes from AFM to FM when U_{eff} is increased from 0 to 3 eV and from 3 to 4 eV, respectively. We find this result very interesting because, even in the case when these methods fail to predict the experimental findings, it could give insight as to how the AFM or FM configurations are established and which are the main orbitals that contribute to the selection of one or the other magnetic state. In fact, by looking carefully at the changes of the electronic structure when employing different exchange-correlation functionals, we were able to identify the main magnetic interactions that are responsible for obtaining the AFM or the FM ground states in the calculations. This study allows us to offer a qualitative explanation for the change in the calculated ground state employing the results for the electronic structure and physical arguments similar to those exposed in the Goodenough-Kanamori-Anderson (GKA) rules.[25–27]

We have found that the decrease of the hybridization of the p_z orbital of oxygen atoms, having sp^2 hybridization (from

now on just p_z *orbital*), with the 3*d* orbitals of manganese, is at the origin of the appearance of the FM ground state and the reduction of the gap for $U_{\text{eff}} \geqslant 2.0$ eV. Since the Mn-O-Mn angles in this compound are 100° and 130° (thus, neither 90° nor 180°), symmetry arguments like those at the basis of the GKA rules[25–27] can not be applied. Still, we rationalize the presence of the AFM and FM ground states by using similar arguments to those described by the GKA rules for high-symmetry orbitals.[28] We argue that the AFM superexchange is mediated by the p_z *orbital*. Both a large-U parameter and a fraction of exact exchange push down in energy the occupied 3*d* states of manganese, thereby disrupting the alignment with the p_z *orbital* and decreasing Mn3*d*-O2*p* hybridization. This phenomenon results in a decrease of the AFM superexchange mediated by the p_z *orbital* leading to a ferromagnetic ground state. As the hybridization decreases, the p_z *orbitals* are destabilized and move up in energy, thereby closing the gap.

The rest of this paper is organized as follows: We explain the computational methods used for this calculations in Sec. II. Then, we study the structural, electronic, and magnetic properties of α-MnO_2 in Sec. III. Finally, conclusions are drawn in Sec IV.

II. COMPUTATIONAL METHODS

All calculations have been performed in the framework of DFT and its extensions, as implemented in QUANTUM-ESPRESSO.[29,30] The generalized-gradient approximation has been employed in the version of PBE,[5] together with Vanderbilt ultrasoft pseudopotentials.[31] The presence of the open 3*d* shell of manganese makes it necessary to test whether standard DFT can properly describe this system. It has been shown that post-DFT methods such as PBE + U and hybrid functionals often describe oxides of manganese better than PBE.[1] In this work, PBE + U (Ref. 32) and hybrid functionals[33,34] were employed as well. PBE + U calculations were performed with the simplified version of Dudarev *et al.*[35] as implemented in the QUANTUM-ESPRESSO code,[36] with different values of U_{eff} ($U_{\text{eff}} = 1.6$, 2.0, and 3.9 eV). The first value was determined as $U_{\text{eff}} = U - J$, as it is usually done in the literature,[37] using the values of U and J from Ref. 20. The value of 3.9 eV was employed in Ref. 22 to study lithium adsorption on α-MnO_2. The value of 2.0 eV was selected because a change in the calculated magnetic ground state was observed for this value. Finally, the hybrid functionals HSE,[24] B3LYP,[38–41] and PBE0 (Refs. 33 and 42) were employed. As the outcome obtained from these hybrid functionals has the same physical implications, here we just show the HSE results.

For the wave functions and the charge density, energy cutoffs of 30 and 300 Ry have been respectively employed in the PBE and PBE + U calculations. A mesh of $(1 \times 6 \times 1)$ k points was necessary for the integration in the first Brillouin zone of the elementary cell. All calculations were performed in a $(1 \times 2 \times 1)$ supercell to allow for AFM ordering along the short y direction, with $(1 \times 3 \times 1)$ k points. Optimizations have been performed for PBE and PBE + U, for all values of U_{eff} considered in this study, until forces were smaller than 10^{-3} a.u. For hybrid functionals, norm-conserving Troullier-Martins pseudopotentials were employed. For this reason, a higher cutoff of 40 Ry was used and only single-point calculations were performed, with the structures relaxed with PBE + U ($U_{\text{eff}} = 1.6$ eV). In practice, the calculation with hybrid functionals was only possible by using the extra level of parallelism, over electronic bands, introduced recently in Ref. 45.

III. RESULTS AND DISCUSSION

A. Structural properties

α-MnO_2 crystallizes in the tetragonal hollandite structure, where the Mn atoms are octahedrically coordinated to six oxygen atoms, as shown in Fig. 1. In this type of lattice, two edge-sharing slightly distorted octahedra are connected in one vertex (vertex-sharing) to form (2×2) channels (see Fig. 1). In the hollandite structure, each oxygen atom is coordinated to three manganese atoms; half of the oxygen atoms have an sp^2 hybridization[17] [O(sp^2)] and lie roughly in the same plane as the three nearest Mn neighbors, while the other half have an sp^3 hybridization[17] [O(sp^3)] and lie out of the plane of the three nearest Mn neighbors [see Fig. 1(b)]. The Mn-O-Mn angles are approximately of 100° and 130° in our calculations. The O(sp^3)'s are the oxygens located at the edge-sharing octahedra in neighboring columns and the closest to the center of the channel while the O(sp^2)'s connect these two edge-sharing octahedra to form the (2×2) channels [see Fig. 1(a)].

The lattice parameters obtained using PBE show a monoclinic distortion from the exact tetragonal structure with $a = 9.89$ Å, $b = 9.75$ Å , and $c = 2.86$ Å. All manganese atoms are in equivalent positions, at the center of an octahedron formed by six oxygen atoms. The octahedra are slightly distorted, with Mn-O distances of 1.90–1.94 Å. The small monoclinic distortion was also reported in a recent work.[20] The cell parameters are in good agreement with those obtained experimentally from x-ray diffraction [$a = 9.750$ Å, $c = 2.861$ Å (Ref. 46)]. The calculated cell parameters are reported in Table I. Relaxing with PBE + U (for $U = 1.6$ eV), the lattice constants change only slightly ($a = 9.92$ Å, $b = 9.80$ Å, $c = 2.90$ Å). We have

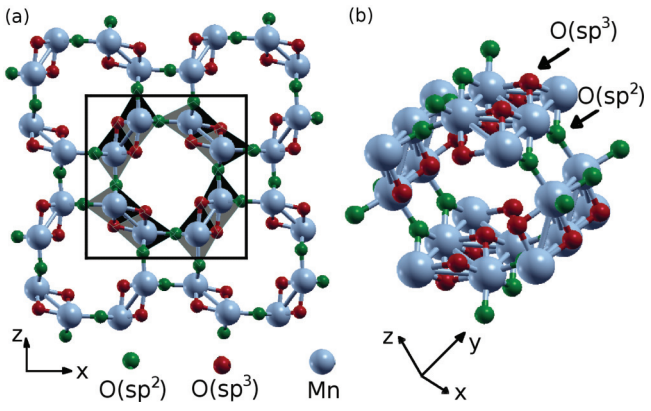

FIG. 1. (Color online) Different views of the hollandite structure for the case of α-MnO_2 compound (Refs. 43 and 44): (a) the xz plane containing the Mn atoms and the two types of oxygen atoms the one with sp^2 hybridization [O(sp^2)] and those with sp^3 hybridization [O(sp^3)]; (b) panoramic view of the channel where the two types of oxygen hybridization can be better observed.

TABLE I. Cell parameters (in Å) for bulk α-MnO_2. The values calculated in this work refer to PBE and to PBE + U (U = 1.6 eV).

	This work		Literature	
	PBE	PBE + U	PBEsol + U	Experiment
a (Å)	9.89	9.92	9.702 (Ref. 20)	9.750 (Ref. 46) 9.784 (Ref. 47)
b (Å)	9.75	9.80	9.685 (Ref. 20)	$b = a$ (Refs. 46 and 47)
c (Å)	2.86	2.90	2.856 (Ref. 20)	2.861 (Ref. 46) 2.863 (Ref. 47)

relaxed the structure with several magnetic configurations (see Sec. III B) and exchange-correlation functionals (PBE, PBE + U with U = 1.6, 2.0, and 3.9 eV), and the differences in the cell parameters were smaller than 1% (see Table II).

B. Electronic and magnetic properties

To find the magnetic ground state, we have investigated several magnetic configurations. We start by considering the possible AFM ground states reported in a recent work for magnetic compounds with the hollandite structure, as α-MnO_2.[48] These configurations are shown in Fig. 2 and consist of (a) C-type antiferromagnetic (C-AFM) with an AFM alignment in the clockwise/counterclockwise direction and a FM along the y direction (*Mn lines*); (b) C2-AFM, composed of two FM *Mn lines* coupled antiferromagnetically; (c) A2-AFM composed of sets of two FM xy planes, with the sets then coupled antiferromagnetically between them; (d) G-AFM with an AFM alignment along the Cartesian directions (in this case the oxygen atoms have been omitted for a better appreciation of the magnetic order). We have also considered a FM arrangement and different realizations where we start from a given configuration of the spins in the xz plane (for example, any of the previous cases) and then keep the AFM alignment along the y direction. We have called the collection of the AFM configurations created by following the previous procedure the "y-AFM family." All methods (PBE, PBE + U, and hybrid functionals) consistently show that the energy difference inside the y-AFM family is one order of magnitude smaller than the difference between the G-AFM configuration

TABLE II. Relative energies of the different magnetic orders (in meV/Mn atom). AFM stands for antiferromagnetic states, FM for ferromagnetic states. Each magnetic configuration was relaxed according to the procedure explained in Sec. II. For a description of the different AFM orders, see text and Fig. 2. The value of the gap [Δ(eV)] for the ground-state configuration is also included.

Magnetic configuration	PBE	PBE + U (1.6 eV)	PBE + U (2.0 eV)	PBE + U (3.9 eV)	HSE
C-AFM	5	29	24	90	124
C2-AFM	0	0	4	49	91
A2-AFM	66	46	42	71	93
xyz-AFM	18	27	31	97	127
FM	46	7	0	0	0
Gap [Δ(eV)]	0.82	0.94	0.93	0.78	2.2

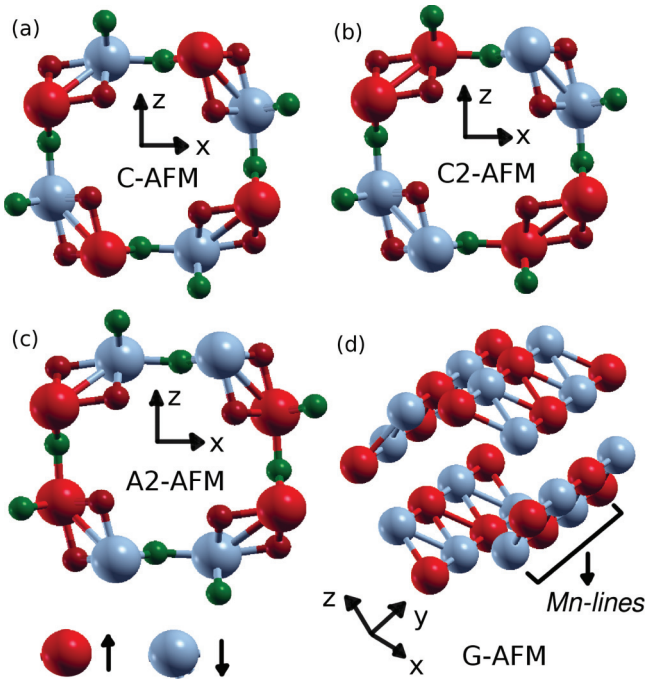

FIG. 2. (Color online) Magnetic configurations studied on the hollandite lattice. (a) C-type antiferromagnetic (C-AFM), with an AFM alignment in the clockwise/counterclockwise direction and a ferromagnetic (FM) along the y direction (*Mn lines*). (b) C2-AFM, composed of two FM *Mn lines* coupled antiferromagnetically. (c) A2-AFM composed of sets of two FM xy planes, the sets are then coupled antiferromagnetically between them. (d) G-AFM, with an AFM alignment along the Cartesian directions (in this case the oxygen atoms have been omitted for a better appreciation of the magnetic order).

[that belongs to the y-AFM-family, see Fig. 2(d)] and the ground state (see Table II). This result implies that the main magnetic interaction is of nearest-neighbor origin, with the three groups of nearest neighbors considered by Crespo *et al.* in Ref. 48 being those that contribute most to the magnetic interaction.

In Table II, the relative energies of the different magnetic orders (in meV/Mn atom) obtained by relaxing the system for all the magnetic configurations are shown. The differences in energy with respect to the ground state increase by 20%–30% if the system is not relaxed with the new magnetic order. Both PBE and PBE + U ($U_{\text{eff}} \leqslant 1.6$ eV) methods find the ground state to be the C2-AFM configuration, as shown in Fig. 2(b). This ground state was also found by Cockayne *et al.*[20] Experimentally, an AFM ground state was observed[2] but the precise direction of the atomic moments has not been reported. However a different picture comes from PBE + U ($U_{\text{eff}} \geqslant$ 2.0 eV) and hybrid functionals where a FM ground state is obtained. A similar change from AFM to FM at increasing U_{eff} had been previously seen for α-Mn_2O_3 and β-MnO_2.[1] All methods consistently find that the ground state of this system is semiconducting with an indirect gap. We did not find any experimental measurement of the gap for undoped α-MnO_2; indeed, in experiments impurities are usually present in the pores. Interestingly, the gap has a nonmonotonic behavior when the value of U_{eff} is increased: it first increases from

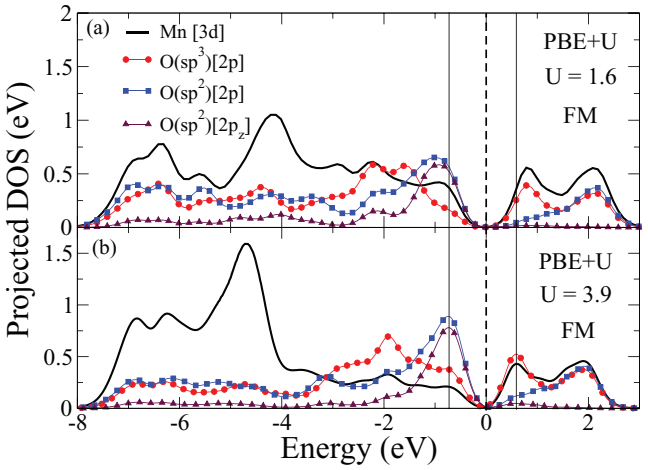

FIG. 3. (Color online) Projected density of states (PDOS) of bulk α-MnO_2, for a FM configuration, calculated with PBE + U with (a) $U_{\text{eff}} = 1.6$ eV and with (b) $U_{\text{eff}} = 3.9$ eV. PDOS of the 3d orbitals of Mn atom: solid line; PDOS of the O(sp^3) atoms: solid line plus filled circles; PDOS of the O(sp^2) atoms: solid line plus filled squares; PDOS of the p_z *orbital* of the O(sp^2) atoms: solid line plus filled triangles. The dashed vertical line indicates the midpoint of the gap. Solid vertical lines are a guide to the eye.

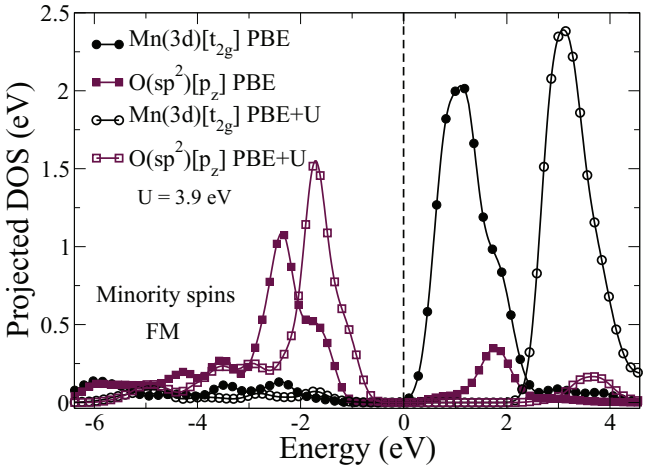

FIG. 4. (Color online) Projected density of states (DOS) for the down spins on the p_z *orbital* of the O(sp^2) atom (multiplied by a factor of 2) and the minority t_{2g} orbitals of Mn(3d) atom, for a FM configuration, calculated with PBE and PBE + U ($U_{\text{eff}} = 3.9$ eV). Four curves are plotted: (i) t_{2g} orbitals (PBE), filled circles; (ii) p_z *orbital* (PBE), filled squares; (iii) t_{2g} orbitals (PBE + U), open circles; (iv) p_z *orbital* (PBE + U), open squares. The dashed vertical line indicates the midpoint of the gap.

$\Delta = 0.82$ eV for PBE to $\Delta = 0.94$ eV for PBE + U, $U_{\text{eff}} = 1.6$ eV, and then it starts to decrease for $U_{\text{eff}} = 2.0$ eV ($\Delta = 0.93$ eV) and $U_{\text{eff}} = 3.9$ eV ($\Delta = 0.78$ eV) (see Table II). This change of the monotonicity of the gap occurs exactly when the ground state becomes FM instead of AFM (see Table II). The gap for the HSE calculations is $\Delta = 2.2$ eV, larger than the one given by the other functionals. This last discrepancy is typical of these methods.[1,49]

To understand this unusual behavior of the gap, we decided to look carefully at the effect that U_{eff} has on the composition of valence and conduction bands. In Fig. 3, the projected DOS (PDOS) is shown for a FM configuration, calculated by PBE + U with (a) $U_{\text{eff}} = 1.6$ eV and (b) $U_{\text{eff}} = 3.9$ eV. The conduction band is dominated by O(2p) of the O atom with sp^3 hybridization and Mn(3d) states. The edge of the valence band moves up, reducing the gap as the value of U_{eff} is increased. The contribution of Mn 3d states to the valence band is moved down when U_{eff} is increased and the major contribution to the edge of the valence band comes from the p_z *orbitals*. The Hubbard U moves down the 3d states of Mn, and thus their hybridization with the p_z *orbitals* decreases (see also Fig. 5). As a consequence, the p_z *orbitals* are destabilized and move up, reducing the gap.

Now, we focus on the question as to why for $U_{\text{eff}} \leqslant 1.6$ eV the ground state is AFM while for $U_{\text{eff}} \geqslant 2.0$ eV we get a FM one. Goodenough-Kanamori-Anderson (GKA) rules[25–27] give a method to determine the type of superexchange interaction for some geometries; for example, when the Mn-O-Mn form an angle of 180° the superexchange interaction is known to be AFM and when the angle is 90° the superexchange is known to be FM.[25–27] In our system, the angles are approximately 100° and 130°, thus GKA rules can not be straightforwardly applied. Furthermore, by increasing U_{eff} the symmetry of the cell does not change, therefore this change can not be explained using just the symmetry of the system.

To answer this question, we study the changes of the electronic structure when employing different exchange-correlation functionals and we notice two main consequences of an increased U_{eff} on the density of states: first, the hybridization of the p_z *orbital* with the Mn 3d orbitals gets reduced. The reduction on the minority spins can be seen from Fig. 4 where we show the PDOS for the down spin on the p_z *orbital* (multiplied by a factor of 2) and the minority t_{2g} orbitals of Mn(3d) atoms, for a FM configuration, calculated with PBE and PBE + U ($U_{\text{eff}} = 3.9$ eV). As it can be seen

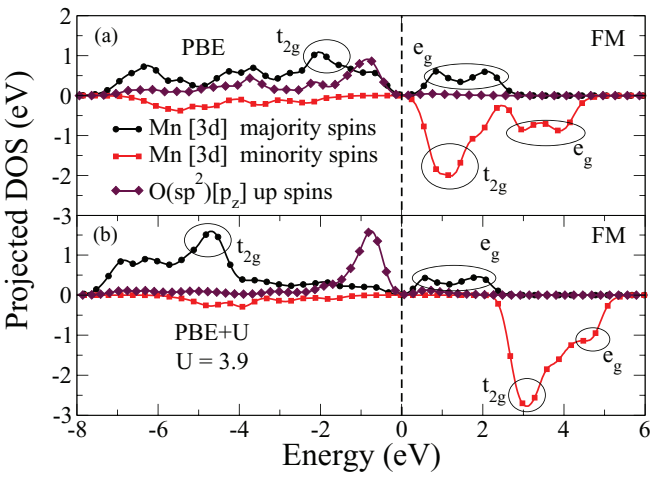

FIG. 5. (Color online) Projected density of states (DOS) of the 3d orbitals of Mn atom and the up spin of the p_z *orbital* of the O(sp^2) atom (multiplied by a factor of 2), for a FM configuration, calculated with (a) PBE, (b) PBE + U ($U_{\text{eff}} = 3.9$ eV). Three curves are plotted: (i) Mn 3d orbitals majority spins (solid line plus filled circles), (ii) Mn 3d orbitals minority spins (solid line plus filled squares), and (iii) the p_z *orbital* (solid line plus filled diamonds). The dashed vertical line indicates the midpoint of the gap.

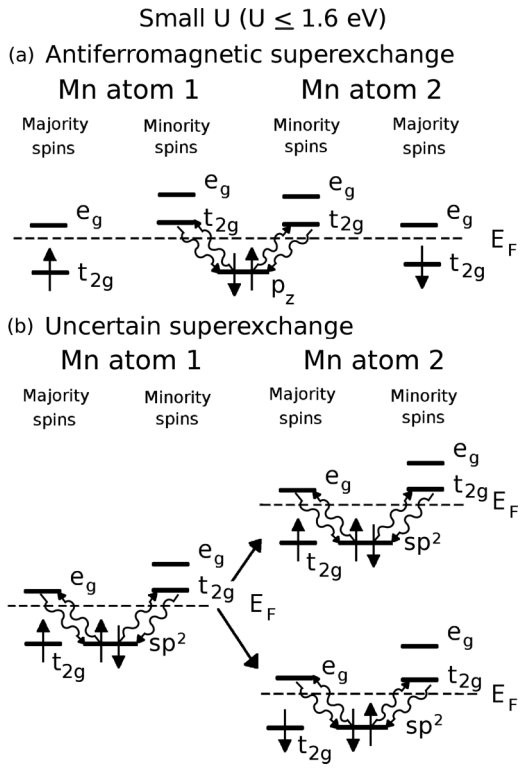

FIG. 6. Diagram of the proposed superexchange interactions between two Mn atoms mediated by the O(sp^2) atoms for $U_{\text{eff}} \leqslant$ 1.6 eV. The total interaction is split into two main contributions: (a) antiferromagnetic superexchange mediated by the p_z*orbital* and (b) uncertain superexchange mediated by the sp^2 orbitals of oxygen. Hybridization is visualized as virtual hopping of electrons as undulated arrows between orbitals.

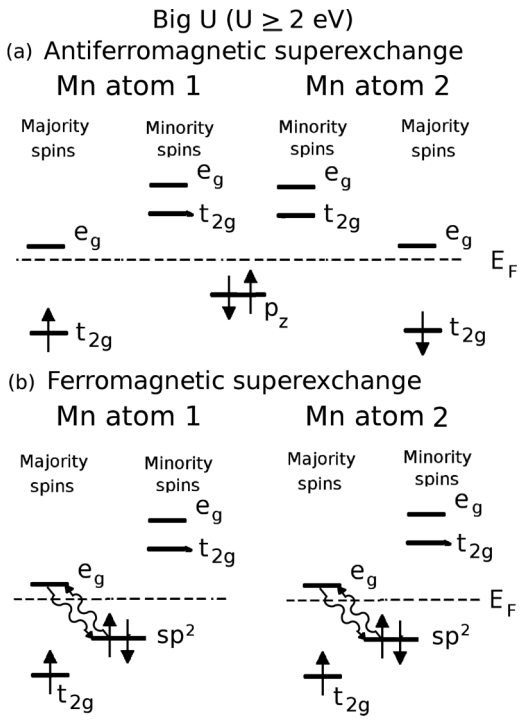

FIG. 7. Diagram of the proposed superexchange interactions with the O(sp^2) atoms for $U_{\text{eff}} \geqslant 2.0$ eV. The total interaction is split into two main contributions: (a) antiferromagnetic superexchange mediated by the p_z *orbital* and (b) ferromagnetic superexchange mediated by the sp^2 orbitals of oxygen. Hybridization is visualized as virtual hopping of electrons as undulated arrows between orbitals. In the case (a), these are not shown to signify that the expected hybridization is small (see text).

from this figure, as the parameter U_{eff} is increased, the minority t_{2g} orbitals move up in energy. At the same time, the contribution of the p_z *orbital* to the formation of common states in the conduction band is reduced. The same is true for the peaks of the minority t_{2g} orbitals that take part in the formation of common states in the valence band. The change in the hybridization of the majority spins is more pronounced (Fig. 5). As the increase of the Hubbard U moves down the t_{2g} orbitals of Mn, their hybridization with the p_z *orbital* gets drastically reduced. As a consequence, the peak corresponding to the p_z *orbital* becomes sharper (see both Figs. 4 and 5). Additionally, the hybridization of the p_z *orbital* with the e_g orbitals of Mn is negligible (they are almost orthogonal). This is confirmed by the absence of peaks in coincidence of the majority e_g orbitals (Figs. 3 and 5). Similar results are obtained also in the case of minority spins (data not shown). The second consequence of increasing U_{eff} is also shown in Fig. 5. In PBE, the t_{2g} orbitals of the majority spins lie below the Fermi energy level (dashed vertical line), while the e_g orbitals of the majority spins and both the t_{2g} orbitals and e_g orbitals of the minority spins are above the Fermi level. When U_{eff} is increased, the t_{2g} orbitals of the majority spins move down in energy while both the t_{2g} orbitals and the e_g orbitals of the minority spins move up in energy [Fig. 5(b)]. In both cases, the occupations of the t_{2g} and e_g orbitals satisfy the Hund's rule for Mn^{4+}.

C. Superexchange mechanism

In general, understanding the magnetic properties of Mn compounds is very difficult because of the multiple possible hybridizations involving the 3*d* orbitals, their high degeneracy, as well as the various possible oxidation states. All these details play an important role in determining the large variety of magnetic properties of MnO_x.[1–4] Therefore, to understand the physics behind the calculated results, it is useful to simplify the problem. In order to rationalize the previous results, we propose the following simplified mechanism for the establishment of the AFM or the FM ground states. First of all, we notice that the superexchange interaction involving the O(sp^3) atoms is always FM in both ground-state configurations (C2-AFM and FM), thus the AFM interaction is mediated by the O(sp^2) atoms. The O(sp^2)'s have four valence orbitals, three sp^2, and one p_z *orbital*. As in both cases (C2-AFM and FM), the *Mn lines* are FM in the y direction we consider only the superexchange between two Mn atoms (on different *Mn lines*) and one oxygen atom. We now assume that the Mn atoms have the oxidation state of Mn^{4+} with the electrons in the t_{2g} orbitals distributed according to the Hund's rule. All assumptions are schematically represented in Figs. 6 and 7.

Let us start by analyzing the case when $U_{\text{eff}} \leqslant 1.6$ eV. First, we study the hybridization of the sp^2 orbitals with the neighboring Mn atoms. Since the whole structure consists of distorted octahedra, the system has no symmetries and therefore the sp^2 and the 3*d* orbitals are never orthogonal.

Without loss of generality, we can assume that in the Mn atom 1 the majority spins have spins up. Then, the sp^2 orbital with spin up can hybridize with the e_g orbitals of the majority spins while the orbital with spin down can hybridize with the t_{2g} orbitals of the minority channel [see Fig. 6(b)]. This situation, where both electrons of the sp^2 orbital can hybridize with a $3d$ orbital of the Mn atom and therefore they can delocalize, brings as a consequence that no magnetic configuration will be preferred by the second Mn atom, which can have a majority of either up or down spins. We have called this an uncertain superexchange interaction [Fig. 6(b)].

We do the same reasoning for the case of the p_z *orbital*. In this case, no hybridization is allowed between the p_z and the e_g orbitals, as explained above. As done previously, we assume that the Mn atom 1 has a majority of up electrons; as a consequence, only the p_z *orbital* with spin down hybridizes with the t_{2g} orbitals (minority). To determine which type of spin will be preferred by the second atom, we notice that this case is very similar, in the physical interpretation, to the case of the 180° exchange of the GKA rules. In that case, the electrons want to delocalize as much as possible; for this reason, they maximized the virtual hopping to neighboring sites decreasing their kinetic energy. As a consequence, an AFM superexchange is obtained.[28] Using the same physical arguments, we argue that a configuration where the up electron of the p_z *orbital* can make hopping with the minority channel of the second Mn atom will be lower in energy and, consequently, the majority channel will be occupied by down electrons, resulting in an AFM superexchange [see Fig. 6(a)]. Since one contribution to the total Mn-Mn interaction is AFM and the other is neither clearly ferromagnetic nor AFM, it is therefore to be expected that the overall interaction is AFM.

Now, we consider the case when $U_{\text{eff}} \geqslant 2.0$ eV, represented in Fig. 7. This time the gap between the orbitals of the O(sp^2) atoms and the t_{2g} orbitals (minority) of the Mn atoms is much larger than the one with e_g orbitals (majority). This situation reduces the hybridization of the p_z *orbital* with the t_{2g} orbitals (minority) of the Mn atoms, as we mention above, and the AFM exchange gets reduced [see Fig. 7(a)]. Furthermore, the hybridization of the sp^2 orbital with the t_{2g} orbitals (minority) of the Mn atoms also becomes smaller and the virtual hopping with e_g orbitals (majority) prevails. As a consequence, if we assume that the Mn atom 1 has up electrons in the majority channel, then the up electron of the sp^2 orbital can make hopping with the e_g orbitals of the majority channel with bigger probability than the down electron. This prevalent presence of the down electrons in the sp^2 orbital implies that a configuration where in the neighbor sp^2 orbital also the down-electron remains will be lower in energy because of the Hund's rules, in a mechanism similar to the 90° exchange of the GKA rules.[28] As a consequence, the superexchange will be ferromagnetic [Fig. 7(b)]. Therefore, the calculated ground state changes from AFM to FM at increasing U_{eff} because the AFM superexchange with the p_z *orbital* gets reduced and the superexchange with the sp^2 orbitals becomes FM.

IV. CONCLUSIONS

The manganese oxide α-MnO_2 with a hollandite structure has been investigated by density functional theory, at the level of the generalized-gradient approximation PBE, with PBE + U ($U_{\text{eff}} = U - J = 1.6$, 2.0, and 3.9 eV) and with the hybrid functionals. All methods consistently predict a semiconducting behavior. Hybrid functionals and PBE + U ($U_{\text{eff}} \geqslant 2.0$ eV) predict a ferromagnetic (FM) configuration as the ground state (see Table II), failing to reproduce the antiferromagnetic (AFM) ground state found in the experiments.[2] If the exchange-correlation functionals PBE and PBE + U ($U_{\text{eff}} \leqslant 1.6$ eV) are employed, then the minimum energy is obtained for the C2-AFM configuration [see Fig. 2(b)]. Even the cases when the calculations fail to predict the experimental findings give insight on how the AFM or FM configurations are established and which are the main orbitals that contribute to the selection of one or the other magnetic ground state. In fact, the careful study of the changes of the electronic structure, when employing different exchange-correlation functionals, makes it possible to identify the main magnetic interaction responsible for getting the AFM or the FM ground states. It also offers a qualitative explanation for the change in the calculated ground state using physical arguments similar to those exposed in the Goodenough-Kanamori-Anderson rules (GKA).[25–28]

In α-MnO_2, two types of oxygen atoms are present: one type with sp^2 hybridization [O(sp^2)] and one with sp^3 hybridization [O(sp^3)] (see Fig. 1). In the DOS, a completely different behavior of these two types of oxygen is seen (see Fig. 3). The superexchange mediated by O(sp^3) type remains FM independently of the functional used and the conduction band is dominated by O(sp^3) and Mn($3d$) states. On the other hand, the p_z *orbitals*, having sp^2 hybridization, dominate the edge of the valence band, and are hybridized with the $3d$ states of manganese. We show that these p_z *orbitals* of oxygen are at the origin of the reduction of the gap for $U_{\text{eff}} \geqslant 2.0$ eV and we argue that they are also responsible for the appearance of both the AFM and the FM calculated ground states. This conclusion is supported by two main results: first, the hybridization of the p_z *orbital* with the e_g orbitals of manganese is negligible (see Fig. 3), and, second, increasing values of U_{eff} push down in energy the $3d$ states of Mn (see Fig. 5). This behavior of the $3d$ states of Mn is responsible for a decrease in the hybridization between the p_z *orbital* and the t_{2g} orbitals as U_{eff} is increased, explaining both the change to a FM ground state and the reduction of the band gap at large values of the Hubbard U. Finally, we have developed a qualitative explanation for the difference on the electronic and magnetic properties obtained with PBE + U in dependence of the value of the Hubbard U based on the previous results and on physical arguments similar to those at the basis of the GKA rules. In this simplified picture, we conclude that the p_z *orbitals* are responsible for the AFM interaction between Mn atoms.

ACKNOWLEDGMENTS

The authors would like to thank E. Tosatti, A. Andreanov, O. Gonzales, and M. Girtu for fruitful discussions. The authors thank I. Girotto for the support with the use of high-performance computing facilities. Computational resources were provided by CINECA, through the ISCRA-C project AFSGMNO2, and by The Abdus Salam ICTP.

[1]C. Franchini, R. Podloucky, J. Paier, M. Marsman, and G. Kresse, Phys. Rev. B **75**, 195128 (2007).
[2]N. Yamamoto, T. Endo, M. Shimada, and T. Takada, Jpn. J. Appl. Phys. **13**, 723 (1974).
[3]H. Sato, J.-I. Yamaura, T. Enoki, and N. Yamamoto, J. Alloys Compd. **262**, 443 (1997).
[4]H. Sato, T. Enoki, J.-I. Yamaura, and N. Yamamoto, Phys. Rev. B **59**, 12836 (1999).
[5]J. P. Perdew, K. Burke, and M. Ernzerhof, Phys. Rev. Lett. **77**, 3865 (1996).
[6]T. Ogasawara, A. Debart, M. Holzapfel, P. Novak, and P. G. Bruce, J. Am. Chem. Soc. **128**, 1390 (2006).
[7]P. G. Bruce, S. A. Freunberger, L. J. Hardwick, and J. M. Tarascon, Nat. Mater. **11**, 19 (2012).
[8]S. A. Freunberger, S. A. Chen, S. A. Peng, J. M. Griffin, L. J. Hardwick, F. Barde, P. Novak, and P. G. Bruce, J. Am. Chem. Soc. **133**, 8040 (2011).
[9]G. Girishkumar, B. McCloskey, A. C. Luntz, S. Swanson, and W. Wilcke, J. Phys. Chem. Lett. **1**, 2193 (2010).
[10]P. Albertus, G. Girishkumar, B. McCloskey, R. S. Sanchez-Carrera, B. Kozinsky, J. Christensen, and A. C. Luntz, J. Electrochem. Soc. **158**, A343 (2011).
[11]M. K. Song, S. Park, F. M. Alamgir, J. Cho, and M. Liu, Mater. Sci. Eng., R **72**, 203 (2011).
[12]H. G. Jung, J. Hassoun, J. B. Park, Y. K. Sun, and B. Scrosati, Nat. Chem. **4**, 579 (2012).
[13]A. Debart, A. J. Paterson, J. Bao, and P. G. Bruce, Angew. Chem. Int. Ed. **47**, 4521 (2008).
[14]A. Kraytsberg and Y. Ein-Eli, J. Power Sources **196**, 886 (2011).
[15]L. B. Ellis, K. T. Lee, and L. F. Nazar, Chem. Mater. **22**, 691 (2010).
[16]Y. Shao, S. Park, J. Xiao, J. G. Zhang, Y. Wang, and J. Liu, ACS Catal. **2**, 844 (2012).
[17]C. Wang, L. Sun, Q. Cao, B. Hu, Z. Huang, and X. Tang, Appl. Catal. B **101**, 598 (2011).
[18]X. Tang, J. Li, and J. Hao, Catal. Commun. **11**, 871 (2010).
[19]V. B. R. Boppana and F. Jiao, Chem. Commun. **47**, 8973 (2011).
[20]E. Cockayne and L. Li, Chem. Phys. Lett. **544**, 53 (2012).
[21]J. P. Perdew, A. Ruzsinszky, G. I. Csonka, O. A. Vydrov, G. E. Scuseria, L. A. Constantin, X. Zhou, and K. Burke, Phys. Rev. Lett. **100**, 136406 (2008).
[22]C. Ling and F. Mizuno, Chem. Mater. **24**, 3943 (2012).
[23]J. Heyd, G. Scuseria, and M. Ernzerhof, J. Chem. Phys. **118**, 8207 (2003).
[24]J. Heyd, G. Scuseria, and M. Ernzerhof, J. Chem. Phys. **124**, 219906 (2006).
[25]J. B. Goodenough, Phys. Rev. **100**, 564 (1955).
[26]J. B. Goodenough, J. Phys. Chem. Solids **6**, 287 (1958).
[27]J. Kanamori, J. Phys. Chem. Solids **10**, 87 (1959).
[28]D. Khomskii, *Spin Electronics*, Lecture Notes in Physics Vol. 569, edited by M. Ziese and M. J. Thornton (Springer, Berlin Heidelberg, 2001), pp. 89–116.
[29]P. Giannozzi, S. Baroni, N. Bonini, M. Calandra, R. Car, C. Cavazzoni, D. Ceresoli, G. L. Chiarotti, M. Cococcioni, and I. Dabo *et al*., J. Phys.: Condens. Matter **21**, 395502 (2009).
[30]S. Scandolo, P. Giannozzi, C. Cavazzoni, S. De Gironcoli, A. Pasquarello, and S. Baroni, Z. Kristallogr. **220**, 574 (2005).
[31]D. Vanderbilt, Phys. Rev. B **41**, 7892 (1990).
[32]V. I. Anisimov, J. Zaanen, and O. K. Andersen, Phys. Rev. B **44**, 943 (1991).
[33]M. Ernzerhof and G. E. Scuseria, J. Chem. Phys. **110**, 5029 (1999).
[34]C. Adamo and V. Barone, J. Chem. Phys. **110**, 6158 (1999).
[35]S. L. Dudarev, G. A. Botton, S. Y. Savrasov, C. J. Humphreys, and A. P. Sutton, Phys. Rev. B **57**, 1505 (1998).
[36]M. Cococcioni and S. de Gironcoli, Phys. Rev. B **71**, 035105 (2005).
[37]Z. Fang, I. V. Solovyev, H. Sawada, and K. Terakura, Phys. Rev. B **59**, 762 (1999).
[38]K. Kim and K. D. Jordan, J. Phys. Chem. **98**, 10089 (1994).
[39]P. J. Stephens, F. J. Devlin, C. F. Chabalowski, and M. J. Frisch, J. Phys. Chem. **98**, 11623 (1994).
[40]A. D. Becke, Phys. Rev. A **38**, 3098 (1988).
[41]C. Lee, W. Yang, and R. G. Parr, Phys. Rev. B **37**, 785 (1988).
[42]J. P. Perdew, M. Ernzerhof, and K. Burke, J. Chem. Phys. **105**, 9982 (1996).
[43]J. Luo, H. Zhu, F. Zhang, J. Liang, G. Rao, J. Li, and Z. Du, J. Appl. Phys. **105**, 093925 (2009).
[44]J. Luo, H. Zhu, J. Liang, G. Rao, J. Li, and Z. Du, J. Phys. Chem. C **114**, 8782 (2010).
[45]N. Varini, D. Ceresoli, L. Martin-Samos, I. Girotto, and C. Cavazzoni, Comput. Phys. Commun. **184**, 1827 (2013).
[46]M. M. Thackeray, Prog. Solid State Chem. **25**, 1 (1997).
[47]J. B. Yang, X. D. Zhou, W. J. James, S. K. Malik, and C. S. Wang, Appl. Phys. Lett. **85**, 3160 (2004).
[48]Y. Crespo, A. Andreanov, and N. Seriani, Phys. Rev. B **88**, 014202 (2013).
[49]J. Paier, M. Marsman, K. Hummer, G. Kresse, I. C. Gerber, and J. G. Angyan, J. Chem. Phys. **124**, 154709 (2006).